Structural and Optical Investigations of SiO_2 Layers Implanted with 100 keV Silicon Negative Ions

[1] S. B.Vishwakarma, [1] S. K. Dubey, [2] R.L. Dubey

[1]Department of physics, University of Mumbai, Vidyanagari, Mumbai-400 098, India
[2]Department of physics, St. Xavier's College, 5 Mahapalika Marg, Mumbai-400 001, India.

Abstract: Thin SiO_2 film of thickness 300 nm grown on p-type silicon substrate was implanted with 100 keV silicon negative ions with fluences varying from 1×10^{15} to 2×10^{17} ions cm^{-2}. The glancing angle X-ray diffraction (GXRD), Ultraviolet visible infrared (UV-Vis-NIR) spectroscopy and Raman scattering techniques have been used to investigate SiO_2 thin film after implantation. GXRD spectra of non-implanted sample showed the presence of a broad peak of SiO_2 between 17.5º and 25º. After implantation, silicon peak at 53.20º corresponding to (311) reflection was observed. The variation in peak intensity with respect to ion fluence revealed the increase in silicon concentration within SiO_2 matrix. The increase in strain value showed the lattice expansion after silicon ions implanted in SiO_2. UV-Vis-NIR spectra showed the decrease in energy band gap value for silicon with increase in the ion fluences. Raman scattering measurements revealed the presence of first order and second order Transverse optical (TO) mode at 520.4 cm^{-1} and 963.06 cm^{-1} respectively. Phonon confinement model was employed to first order Raman TO phonon mode revealed the increase in phonon coherence length from 9.41 to 10.04 nm with increase in the concentration of silicon ions in SiO_2 matrix.

Index Terms **–** SiO_2 thin film; GXRD; UV-Vis-NIR; Raman.

I. INTRODUCTION

Microelectronic industry is dominated by silicon for all its microchip technology but for photonic devices, silicon is found incompatible as it has an indirect band gap nature. Then, the discovery of strong luminescence of nanoporous silicon has triggered the need for silicon based photonic devices [1, 2]. The key requirement of photonic devices is shorter radiative lifetime of excited carriers; whereas, silicon has longer radiative lifetime due to indirect band gap nature, which leads to a non-radiative recombination of excited carriers [3]. These limitations may be overcome when silicon nanocrystals (Si-nc) are embedded in a SiO_2 matrix using ion implantation [4]. The physical mechanism responsible for the photoluminescence in Si-nc is quantum confinement of excitons (electron-hole pair) along with light amplification which is possible using silicon as quantum dots dispersed in SiO_2 matrix by ion implantation [5, 6]. It is also commonly accepted, that radiative recombination of carriers at Si-nc/SiO_2 interface plays an important role for light emission [7]. The Si-O vibrations at the Si-nc/SiO_2 interface are supposed to be the dominant path for the recombination of excitons and it is found that the interface is not sharp, but there is some transition region having amorphous silicon and strained SiO_2 network around Si-nc leading to some optically active states [8].

The penetration depth of the silicon ions in SiO_2 thin film is affected by positive ion implantation as the surface of SiO_2 thin film layer gets charged up [9]. Fabrication of MOSFETs is troublesome using silicon positive ion implantation because of the surface breakdown of SiO_2 thin film. Further investigations of atomic structure become tedious work under positive ion implantation.

These limitations of positive ion implantation may be overcome with silicon negative ion implantation. In negative ion implantation, the surface charging effect of the sample is almost negligible, low surface charging effect avoids the breakdown of the insulator which is most effective in field effect transistors as well as in thin film transistors and the atomic bonding processes due to kinetic energy (kinetic bonding) can be efficiently studied because negative ions have small potential energy (electron affinity) [10, 11].

In the present work, SiO_2 thin film is implanted with 100 keV silicon negative ions for the various ion fluences varying from 1×10^{15} to 2×10^{17} ions cm^{-2}. This paper aims to provide a better understanding of the implantation effects produced in SiO_2 thin film using GXRD, UV-Vis-NIR and Raman spectroscopy techniques prior to thermal treatments.

.

II. EXPERIMENTAL DETAILS

The SiO_2 thin films of thickness 300 nm were grown on P-type silicon (100) substrates by dry thermal oxidation method in a furnace at 900 ºC. The samples were cleaned using RCA-1 and rinsed in DI water for removing all the contaminations from the surface. Further samples were dried using an infrared dryer lamp. Thereafter, samples were loaded in the target chamber and implantation had been done with silicon negative ions at 100 keV with fluences 1×10^{15}, 5×10^{15}, 1×10^{16}, 5×10^{16} , 1×10^{17} and 2×10^{17} ions cm^{-2} using Negative Ions by Caesium Sputtering (SNICS) source at Inter University Accelerator Centre (IUAC), New Delhi. The beam was scanned over the area of 1 cm × 1 cm on sample surface for uniformed implantation. The beam current was held at 2 µA during the implantation. Target chamber was maintained at 10^{-6} mbar. The projected range of 100 keV silicon negative ions in SiO_2 films was estimated by Stopping and Range of Ions in Matter (SRIM) software and it was found to be 171.50 nm with longitudinal straggling range up to 54.80 nm [12]. The GXRD measurements were performed at an incidence angle of 1º with respect to the sample surface using a diffractometer RIGAKU-ULTIMA-IV equipped with Cu $K\alpha_1$(λ=0.154 nm) source at the Department of Physics, University of Mumbai. UV-Vis-NIR spectroscopic measurements for non- implanted and all implanted samples were done using spectrophotometer [UH-4150] in the spectral region of 200 to 1200 nm with scan speed of 300 nm/min at IUAC, New Delhi. Raman spectroscopic measurements were performed on RENISHAW inVia Raman microscope at room temperature at IUAC, New Delhi. The excitation was done with 514 nm line of an Ar+ ion laser.

III. RESULTS AND DISCUSSION

GXRD spectra recorded at an incidence angle of 1º for non-implanted sample and samples implanted with 1 ×10 ^{15}, 5 ×10 ^{15}, 1 ×10 ^{16}, 5 ×10 ^{16}, 1 ×10 ^{17} and 2 × 10^{17} ions cm^{-2} are shown in Fig 1(a), 1(b), 1(c), 1(d), 1(e), 1(f) and 1(g) respectively. Fig showed the presence of two peaks at 21.2º and 53.20º in different graphs. The peak at 21.2º is the characteristic peak of SiO_2 shown in first graph [13]. The intensity of the GXRD peak observed at 21.2º decreased up to ion fluence 1 × 10^{16} ions cm^{-2} and disappeared after the ion fluence 5 × 10^{16} ions cm^{-2} indicated the lattice distortion created in SiO_2 at higher ion fluences. The GXRD peak at 53.20º occurred due to the presence of silicon in SiO_2 thin film with interplanar spacing of d~0.177 nm corresponds to (311) reflection. After, the incorporation of silicon ions the peak intensity decreased for the ion fluence of 1 ×10 ^{15} ions cm^{-2}, which may be due to the beginning of structural breakdown. The peak observed at 53.20º shifted towards lower angle for ion fluences upto 5 ×10 ^{16}, which was due to the strain developed as a consequence of increased silicon ions concentration within the lattice of SiO_2 layer. Fig.2 showed the variations of induced strain as a function of ion fluences. The strain was found to increase with the increase in ion fluences but for the ion fluence 1×10 ^{17} ions cm^{-2}, there is a peak shift towards higher angle giving compressive strain, and this may be due to the saturation of silicon concentration within SiO_2 layer. The strain value was evaluated using the following relation,

$$\text{Strain}(\varepsilon) = |d_o \sim d|/d, \quad (1)$$

where d_o and d are interplanar spacing for non-implanted and implanted samples respectively. Here, interplanar spacing was experimentally determined using the following Bragg's relation,

$$2\, d \sin\theta = n\,\lambda, \quad (2)$$

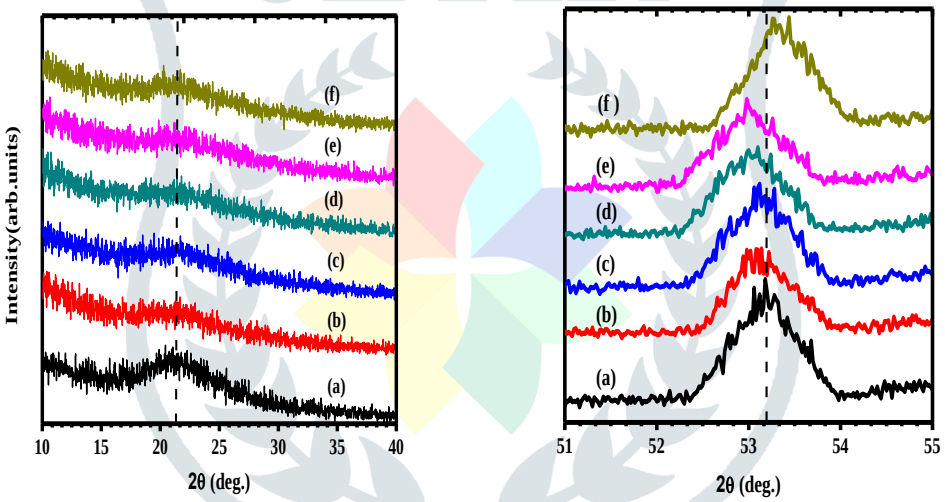

Fig.1. GXRD spectra of SiO_2 at 1º (a) non-implanted and implanted with 100 keV Si negative ions (b) 1×10 ^{15} (c) 5×10 ^{15} (d) 1×10 ^{16} (e) 5×10 ^{16} and (f) 1×10 ^{17} ions cm^{-2}.

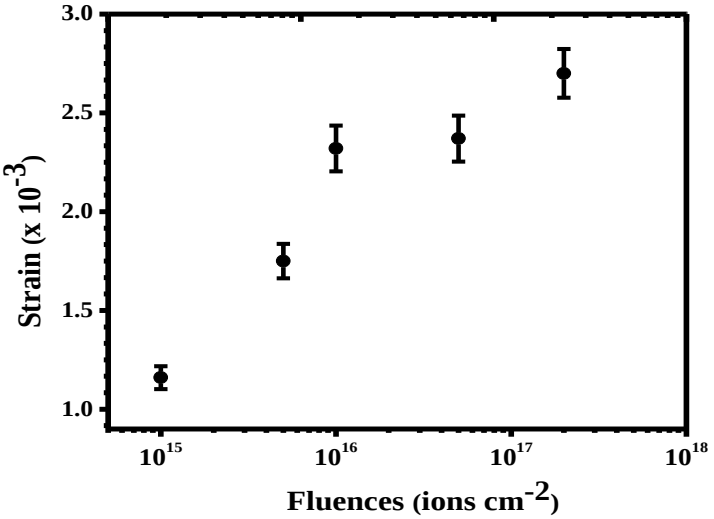

Fig. 2. Strain developed in SiO_2 matrix as a function of ion fluences.

Fig.3 shows the UV-Vis-NIR transmittance spectrum of non-implanted sample and samples implanted with the ion fluences varying from 1×10^{15} to 2×10^{17} ions cm^{-2}. When, light is incident on non-implanted SiO_2 thin film, the light is transmitted into the film and begins to interact with the electronic structure of silicon and creates transition from valence band to conduction band, which cause absorption in the infrared region at the wavelength around 1100 nm [14]. It can be seen that the transmittance value is maximum for the non-implanted sample and for implanted samples it decreased non-uniformly with increase in the ion fluence. This decrease may arise due to an increase in absorption associated with the creation of intermediate energy levels after implantation of silicon negative ions into SiO_2 thin film matrix. Absorption coefficient (α) was calculated using Lambert's law [15], which accounts for the transmission effects. The relation is given as:

$$\alpha = ln(\frac{100}{T})/t \quad (3)$$

Where't' is the thickness of the film and T is the transmittance.

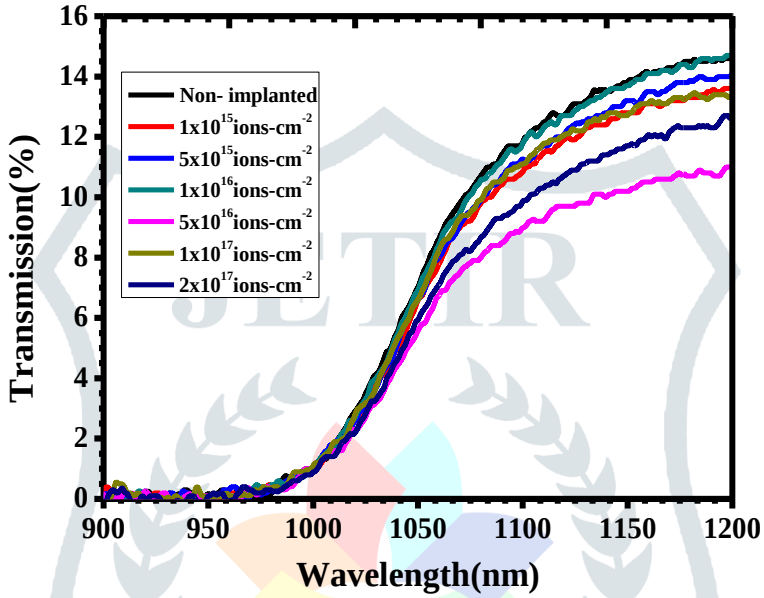

Fig. 3. Transmittance (%T) spectra of non- implanted and implanted SiO_2 with100 keV Si negative ions varying from $1x10^{15}$ to $2x10^{17}$ ions cm^{-2}.

Fig.4 shows the band gap variation of silicon negative ions implanted SiO_2 with the different ion fluences varying from 1×10^{15} to 2×10^{17} ions cm^{-2}. It is observed from the figure that there is no considerable change in the band gap value after implantation, whereas a slight decrement in the band gap value of implanted samples have been observed as compared to non-implanted sample. This effect is due to the breakdown of Si-O bonds creating some defects centers like oxygen vacancies and E'centers as a result of increase in silicon composition after implantation within SiO_2 matrix. The band gap value was calculated by using the method of Tauc-plot, where $(\alpha h\nu)^{\frac{1}{2}}$ was plotted as a function of photon energy $(h\nu)$ for indirect transitions as shown in fig.4. The band gap is determined from the intersection of the tangents on photon energy axis. For, indirect transitions band gap was estimated using the relation:

$$(\alpha h\nu)^{\frac{1}{2}} = B\left(h\nu - E_{gi}\right) \quad (4)$$

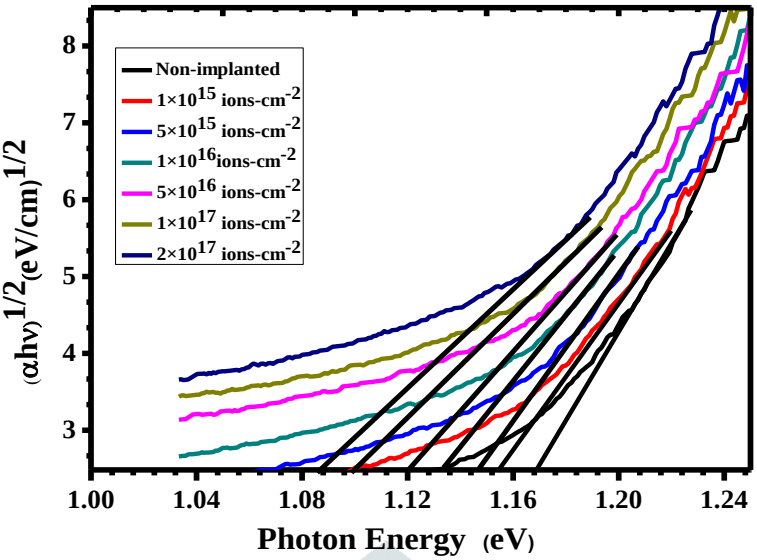

Fig. 4. Energy band gap E_g of non- implanted and implanted SiO_2 with100 keV Si negative ions varying from $1x10^{15}$ to $2x10^{17}$ ions cm^{-2}.

Fig. 5 shows the first order Raman spectra of non- implanted and implanted samples with the ion fluences 1×10^{15} and 1×10^{16} ions cm^{-2}. There is a strong peak observed at 520.4 cm^{-1} due to silicon present in thin SiO_2 layer attributed to the first order transverse optical (TO) mode of silicon [16]. Shift in the Raman peaks towards a higher wave number and broadening of Raman peaks after implantation is attributed to compressive stress and the phonon confinement effects respectively [17].

The approximate magnitudes of the stress (σ) were calculated by using following relation,

$$\sigma(MPa) = -250\Delta\omega\ (cm^{-1}), \tag{5}$$

where $\Delta\omega = \omega_s - \omega_0$, ω_s and ω_0 are the wave numbers of implanted and non-implanted samples respectively. The values of stress were found to be 135 MPa and 87.25 MPa for the ion fluences of 1×10^{15} and 1×10^{16} ions cm^{-2} respectively. The decrease in the compressive stress was found due to defects and disorder produced with increasing ion fluences.

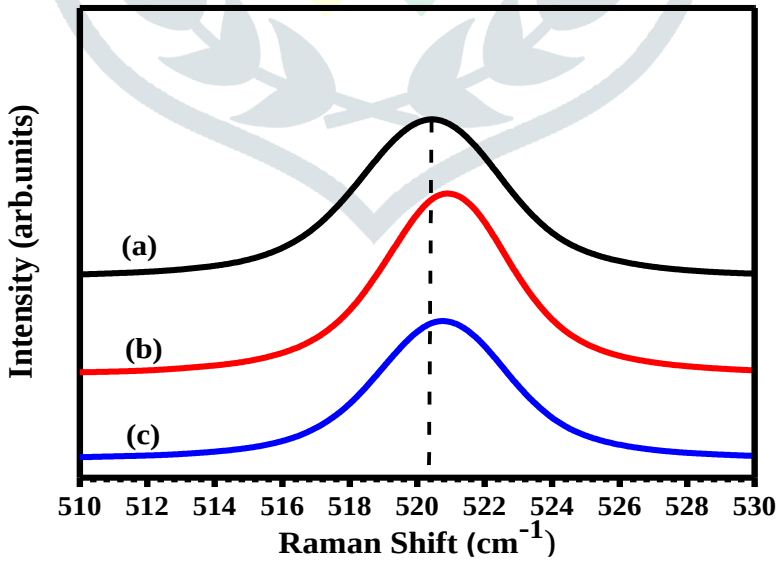

Fig. 5. First order Raman spectrum of SiO_2 (a) Non- implanted and implanted with 100 keV Si negative ions (b) 1×10^{15} and (c) 1×10^{16} ions cm^{-2}.

Fig.6 shows a broad Raman peak at 963.06 cm^{-1} with lower intensity compared to the first order TO Raman mode, this is attributed to the second order TO phonon mode of silicon present in SiO_2 layer [18]. The shift in the peak positions of implanted samples and broadening of the peaks as compared to non-implanted sample resulted as a consequence of silicon ions occupies the interstitials of SiO_2 matrix. There is another Raman peak observed at 1123.76 cm^{-1} that corresponds to SiO_2 thin film layer as

reported by Pawel *et al.* [19]. It is known that SiO_2 group in a rigid framework has vibrational degrees of freedom for Si and O atoms, these peaks correspond to the stretching mode of Si-O-Si bonding [20, 21]. It is also observed that the intensity of the peaks at 1123.76 cm^{-1}, increases with the increase in the ion fluences and there is a shift towards a higher wave number which is attributed to the structural defects such as nonbridging oxygen and hole centers (NBOHC) produced in SiO_2 matrix after the ion implantation [22].

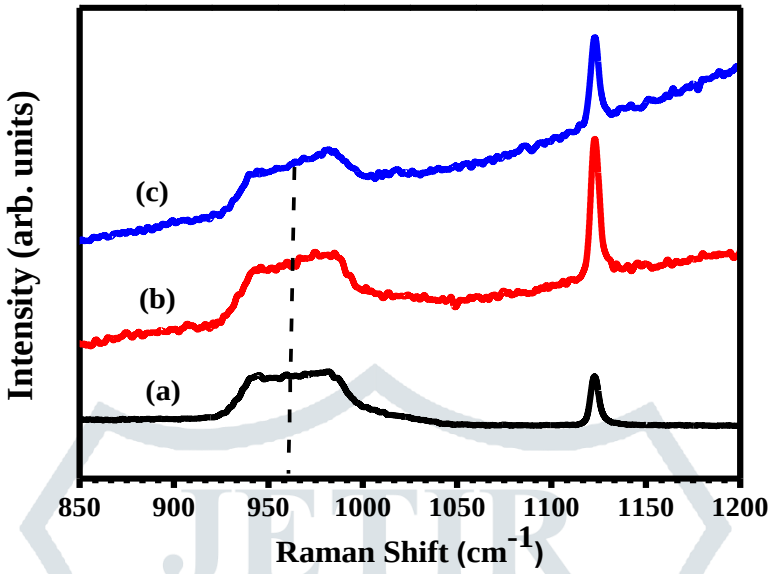

Fig. 6. Second order Raman spectrum of SiO_2 (a) Non- implanted and implanted with100 keV Si negative ions (b) 1×10^{15} and (c) 1×10^{16} ions cm^{-2}.

Fig.7 shows the experimental and PCM fitted first order Raman spectra of ion fluence 1×10^{15} ions cm^{-2} and 1×10^{16} ions cm^{-2}. The Raman TO mode of non-implanted sample is symmetric with an infinite phonon coherence length due to long range periodicity of silicon ions in SiO_2 matrix [23]. After the implantation of silicon negative ions there may be some ion induced effects within SiO_2 matrix, leading to the stress developed in the structure and formation of Si-clusters as a consequence of silicon ions agglomeration [24]. There are different models have been developed, among them a simple and effective phonon confinement model proposed by Richter *et al*. has become the most widely used model in which a wave packet concept and a Gaussian envelope function is used [25, 26]. Using PCM model phonon coherence lengths of 9.4 nm and 10 nm were obtained for the ion fluences 1×10^{15} ions cm^{-2} and 1×10^{16} ions cm^{-2} respectively. This may possibly correspond to the silicon clusters of 9.4 nm and 10 nm sizes produced within SiO_2 thin layer due to local area temperature rise during implantation process.

The intensity of the first-order Raman mode is given by the following relation,

$$I(\omega) = \int_0^{2\pi/a_0} \exp(-q^2L^2/16\pi^2)4\pi q^2\, dq/[\omega - \omega(q)]^2 + \left(\frac{\Gamma_0}{2}\right)^2, \quad (6)$$

where $\omega(q)$ is the phonon dispersion curve, a_0 = 0.543 nm is the lattice constant of silicon, $\Gamma_0 = 3.5\ cm^{-1}$ is the natural line width of crystalline silicon and q is the phonon wave vector expressed in $2\pi/a_0$ units. Assuming a constant coherence length (L) in the scattering volume, the intensity of the first-order Raman mode was estimated using the above equation. To carry out the integration of intensity formula, we have used an isotropic form of phonon dispersion relation for silicon as follows.

$$\omega(q) = [(A - B(qa_0/2\pi)^2)]^2, \quad (7)$$

where $A = 521\ cm^{-1}$ and $B = 120\ cm^{-1}$ are constant for silicon [27].

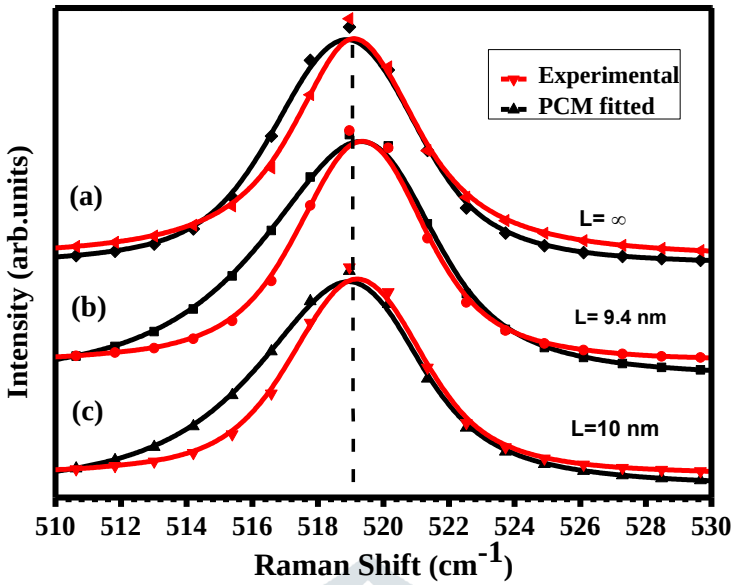

Fig. 7. First order TO Raman mode of silicon implanted in SiO_2 fitted with PCM model for samples (a) Non- implanted and implanted with (b) 1×10^{15} and (c) 1×10^{16} ions cm^{-2}.

IV. CONCLUSIONS

The implantation of SiO_2 thin films by silicon negative ions of energy 100 keV with the various ion fluences varying from 1×10^{15} to 2×10^{17} ions cm^{-2} was carried out. GXRD study revealed the strain developed in SiO_2 thin film layer as a result of increase in silicon concentration after implantation. UV-Vis-NIR studies revealed the decrement in the transmission of incident radiation after implantation and the decrease in the energy band gap value for silicon with increase in the ion fluences. Raman scattering measurements showed first order TO mode at 520.4 cm^{-1}, second order TO mode at 963.06 cm^{-1} and the Si-O-Si stretching mode at 1123.76 cm^{-1}. The shift in the Raman peak showed the presence of stress due to implantation. Phonon confinement model was fitted with experimental results indicated the formation of silicon clusters.

V. ACKNOWLEDGMENTS

The authors are thankful for the financial support received from IUAC, New Delhi, under the AUC-61507 scheme and to the members of the Low Energy Ion Beam Facility (LEIBF) group for providing silicon negative ion beam.

REFERENCES

[1] L. T. Canham, Appl. Phys. Lett. **57**, 1045-1048 (1990).
[2] A. G. Cullis & L. T. Canham, Nature **353**, 335-338 (1991).
[3] Sioma Debela Gosa and S. K. Goshal, Lat. Am. J. Phys. Educ. **6 (2)**, 306-310 (2012).
[4] M. S. Dunaevski, J. J. Grob, A.G. Zabrodski, R. Laiho and A. N. Titkov, Semiconductors **38(11)**, 1254-1259 (2004).
[5] Z. H. Lu, D. J. Lockwood &, J. M. Bari beau, Nature **378**, 258-260 (1995).
[6] L. Pavesi, L. Dal Negro, C. Mazzoleni, G. Franzoa and F. Priolo, Nature **408**, 440-444 (2000).
[7] M. V. Wolkin, J. Jorne, P. M. Fauchet, G. Allan & C. Delerue, Phys. Rev. Lett. **82**, 197-200 (1999).
[8] N. Daldosso, M. Luppi, S. Ossicini, E. Degoli, R. Magri, G. Dalba & P. Fornasini, Phys. Rev. B **68**, 085327(1-8) (2003).
[9] H. Tsuji, N. Arai, N. Gotoh, T. Okumine and J. Ishikawa, Rev. of Sci. Instr. **77**, 03A510 (2006) .
[10] Junzo Ishikawa, Surface and Coatings Tech. **65**, 64-70 (1994).
[11] Junzo Ishikawa, Review of scientific instruments **71**, 1036-1041 (2000).
[12] J.F. Ziegler, M.D. Ziegler, Biersack, Nucl. Instr. Meth. Phys. Res. B **268** (2010).
[13] C.S. Ferreira, P. L. Santos, J. A. Bonacin, R. R. Passos, L. A. Pocrifka ,Materials Research **18(3)** , 639-643 (2015).
[14] Al-Sharafi, S.Mohyeddine, S. O. Mohammed and R.M.Kershi, Physics Research International- **2014**, 594968-1-7 (2014).
[15] D.F. Swinehart, J.Chem.Edu. **39(7)**, 333 (1962).
[16] N. Saxena, P. Kumar, D. Kabiraj and D. Kanjilal, Nanoscale Res. Lett. **547**, 1-7 (2012).
[17] P.K. Giri, R. Kesavamoorthy, S. Bhattacharya, B.K. Panigrahi and K.G.M. Nair, Mat. Sc. & Eng. B **128**, 201–204 (2006).
[18] P. Mishra and K. P. Jain, Physical Rev. **64**, 073304 (2001).
[19] P. Borowicz, M. Latek, and W. Rzodkiewicz, Adv. Nat. Sci. Nanosci. Nanotech. **3**, 045003 (2012).
[20] E. R. Lippincott, A.V.Valkenburg, C. E.Weir and E. N. Bunting, Jour. of Res. of the Nati. Burea of Std. **61**, 61-66 (1958).

[21] Motonari Tsubaki and Nai-Teng Yu, Proc.Natl.Acad.Sci.USA **78**, 3581-3585. (1981).
[22] M. Ya. Valakh, V.A. Yukhimchuk, V. Ya. Bratus and A. A. Konchits, J.Appl. Phys. **85(1)**, 168-173 (1999).
[23] R. L. Dubey, S.K. Dubey, A.D Yadav and D. Kanjilal, Rad. Effs. & Defs. in Solids, 1-6 (2013).
[24] J Alberto Luna Lopez, J Carrillo Lopez, D E Vazquez Valerdi, Nanoscale Research Letters **7**, 604 (2012).
[25] H. Ritcher, Z. P. Wang and L. Ley, Solid State Communications **39**, 625-629 (1981).
[26] Pengfei Zhang, Yu Feng, R. Anthony, U. Kortshagen, G. Conibeer and S Huang, J. Raman Spect. **46**, 1110-1116 (2015).
[27] Claudia R. B. Miranda, Patricia G. Abramof, Francisco C. L. de Melo, Neidenei G. Ferreira, Mat. Res. **7**, 619-623 (2004).